Formation of microtubule-based traps controls the sorting and concentration of vesicles to restricted sites of regenerating neurons after axotomy

Hadas Erez,[1] Guy Malkinson,[1] Masha Prager-Khoutorsky,[1] Chris I. De Zeeuw,[2] Casper C. Hoogenraad,[2] and Micha E. Spira[1]

[1]Department of Neurobiology, Institute of Life Science, The Hebrew University of Jerusalem, Jerusalem 91904, Israel
[2]Department of Neuroscience, Erasmus Medical Center, 3000 DR Rotterdam, Netherlands

Transformation of a transected axonal tip into a growth cone (GC) is a critical step in the cascade leading to neuronal regeneration. Critical to the regrowth is the supply and concentration of vesicles at restricted sites along the cut axon. The mechanisms underlying these processes are largely unknown. Using online confocal imaging of transected, cultured *Aplysia californica* neurons, we report that axotomy leads to reorientation of the microtubule (MT) polarities and formation of two distinct MT-based vesicle traps at the cut axonal end. Approximately 100 μm proximal to the cut end, a selective trap for anterogradely transported vesicles is formed, which is the plus end trap. Distally, a minus end trap is formed that exclusively captures retrogradely transported vesicles. The concentration of anterogradely transported vesicles in the former trap optimizes the formation of a GC after axotomy.

Introduction

The rapid transition of a stationary axonal structure into a motile growth cone (GC) after axotomy involves massive restructuring of the cytoskeleton (Spira et al., 2003; Sahly et al., 2006), the recruitment and localization of membrane resources, and their insertion into the plasma membrane (Ashery et al., 1996; Spira et al., 2003; Sahly et al., 2006). Although the sequence of microtubules (MTs) and actin network restructuring after axotomy was recently analyzed (Spira et al., 2003; Sahly et al., 2006), the mechanisms that regulate vesicle accumulation at the cut axonal end did not receive much attention. This is probably the result of the intuitive assumption that after axotomy, vesicles accumulate at the tips of the disrupted MTs simply because they cannot move efficiently beyond this point.

Earlier studies revealed that axotomy is associated with massive membrane retrieval along the plasma membrane of the cut axonal end. The retrieved membrane appears to serve as part of the resealing mechanism in a variety of neurons (Ziv and Spira, 1995; Ashery et al., 1996; Fishman and Bittner, 2003; Yoo et al., 2004; Nguyen et al., 2005). Whole cell patch-clamp membrane capacitance measurements revealed that the axotomy of cultured *Aplysia californica* neurons activates two processes in parallel: membrane retrieval and exocytosis. Surprisingly, it was demonstrated that axotomy-induced membrane retrieval quantitatively dominates exocytosis for >1 h after axotomy. Thus, although vigorous extension of a GC's lamellipodium was visualized, the total membrane surface area of the neuron decreased (Ashery et al., 1996). These observations implied that in order to permit effective extension of a lamellipodium after axotomy, the sites of membrane retrieval and exocytosis must be spatially separate.

Attempts to determine the site of membrane insertion and retrieval in neurons yielded conflicting results. For example, Popov et al. (1993) suggested that membrane is added along the neurites of cultured *Xenopus laevis* neurons. On the other hand, Dai and Sheetz (1995) and Zakharenko and Popov (1998) concluded that new membrane is added to the GC and that bulk membrane endocytosis occurs in the cell body. To the best of our knowledge, no information is available on the budgeting and spatial distribution of membrane resources or about retrieval and exocytosis in regenerating neurons after mechanical injury.

Using cultured *A. californica* neurons, we report novel mechanisms that rapidly subdivide the cut axonal end into two structurally and functionally distinct compartments. In one compartment, Golgi-derived anterogradely transported vesicles accumulate and fuse with the plasma membrane in support of GC extension; in the other, retrieved plasma membrane is retained. We demonstrate that formation of the two compartments

Correspondence to Micha E. Spira: spira@cc.huji.ac.il

Abbreviations used in this paper: BFA, brefeldin A; DZ, distal zone; EHNA, erythro-9-(2-hydroxy-3-nonyl)adenine; EYFP, enhanced YFP; GC, growth cone; GCOC, GC organizing center; MT, microtubule; PZ, proximal zone; SR101, sulforhodamine 101.

The online version of this article contains supplemental material.

The Journal of Cell Biology, Vol. 176, No. 4, February 12, 2007 497–507
http://www.jcb.org/cgi/doi/10.1083/jcb.200607098

is generated by reorientation of the MT polarities at the cut axonal end. Our observations suggest that formation of the MT-based vesicle traps optimizes the rapid transformation of an axon into a motile GC after axotomy by sorting and concentrating different membrane resources to restricted sites on the cut axon.

Results

Light microscope analysis of cultured *A. californica* neurons showed that axotomy is followed by the formation of a large GC at the tip of the proximal axonal segment (Fig. 1). In the course of 5–15 min after axotomy, a small axonal segment located some 50–150 μm proximal to the cut end swells. We refer to this segment as the GC organizing center (GCOC; Fig. 1 C). The GCOC fills up with organelles and forms the center around which the nascent GC extends (Fig. 1, D and E; Spira et al., 2003; Sahly et al., 2006). The segment located proximally to the swelling (proximal zone [PZ]) retains its cylindrical shape (Fig. 1 C), whereas distal to the GCOC, the axon gradually retracts and assumes a flat form (distal zone [DZ]; Fig. 1 C; Spira et al., 2003). 10–30 min after axotomy, a flat lamellipodium extends laterally from the GCOC (Fig. 1, D and E).

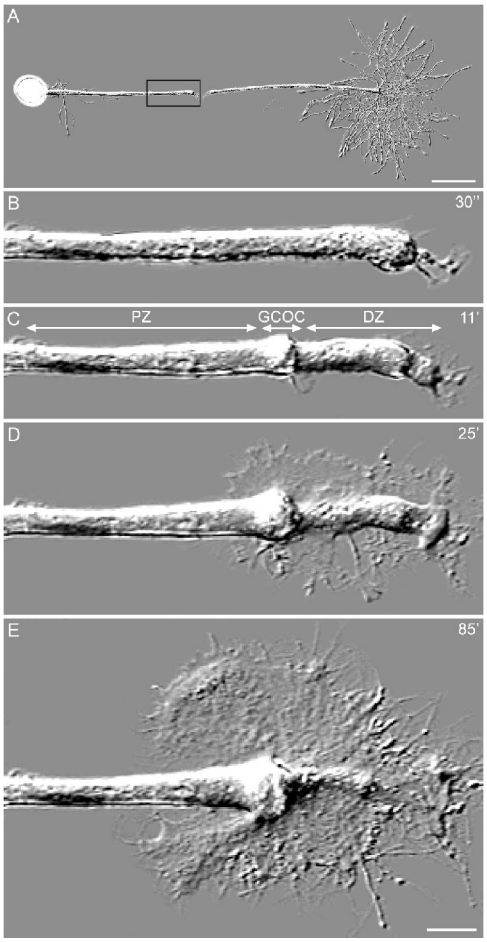

Figure 1. **The morphological sequence of axonal transformation into a GC after axotomy.** (A) A B neuron was cultured for 24 h and transected with a micropipette. (B) After axonal transection, a membrane seal is formed over the cut axonal end. (C) Within 5 min of axotomy, a compartment located ~75 μm proximally to the cut end of the axon swells. This swollen zone, which is referred to as the GC organizing center (GCOC), subdivides the axon into a distal zone (DZ) and a proximal zone (PZ). (D) The GCOC is the area from which the GC's lamellipodium extends. (E) With time, the DZ retracts. The time after axotomy is given in minutes on the right side of the images. B–E are enlargements of the proximal cut end, which is indicated by the boxed area in A. Bars (A), 200 μm; (B–E), 25 μm.

Formation of MT-based vesicle traps by reorientation of MT polarity

To determine what mechanism underlies the accumulation of vesicles in the GCOC, we labeled the dynamic MTs by intracellular microinjection of mRNA encoding GFP-tagged EB3 (end-binding protein 3; Nakagawa et al., 2000; Stepanova et al., 2003), a neuronal MT plus end–tracking protein that accumulates at the distal ends of growing MTs (Stepanova et al., 2003; Akhmanova and Hoogenraad, 2005; Ahmad et al., 2006; Kim and Chang, 2006). These EB3-based fusion proteins transiently bind to the plus end of MTs and move with the growing MT's tips, forming a comet tail–like structure, which allowed us to image the polarity of MTs. Online confocal imaging of intact cultured neurons expressing EB3-GFP revealed that all MTs within the axon and its neurites orient their plus ends distally (Fig. 2 A and Video 1, available at http://www.jcb.org/cgi/content/full/jcb.200607098/DC1). Axotomy leads within seconds to (1) a retrograde wave of EB3-GFP comet tail dissipation from the distal axonal zone (Fig. 2 A2 and Video 1). This wave temporally and spatially corresponds to MT depolymerization, as revealed in studies using imaging of tetramethyl-rhodamine tubulin–labeled MTs (Spira et al., 2003; Sahly et al., 2006). The MT depolymerization wave ends when the cut axonal end reseals, and the free intraaxonal calcium concentration recovers to its resting level (Spira et al., 1993; Ziv and Spira, 1995, 1997). (2) Termination of the EB3-GFP comet tail dissipation wave is followed within minutes of axotomy by an anterograde wave of EB3-GFP comet tail reformation (Fig. 2 A3 and Video 1). Within minutes of axotomy, the MTs at the cut axonal end are restructured in the following manner. In the PZ, all MTs point their plus ends anterogradely (Fig. 2, A4–A7; and see Fig. 8). Distally, the polarity of the MTs reverses such that the plus ends point retrogradely (Fig. 2, A4–A6; and see Fig. 8). This reversal of MT polarity creates the narrow GCOC, which is bordered both proximally and distally by the MT plus ends (plus end trap; Fig. 2, A4–A7; and see Fig. 8). Distal to the GCOC, the MT plus ends point toward the plasma membrane at the tip of the cut axon or are aligned in parallel and close to the plasma membrane (Fig. 2, A4–A6 and A8; and see Fig. 8). This MT orientation forms a second zone, which is bordered by the minus ends of the MTs at the very tip of the cut axon and by the minus ends of the MTs that also border the GCOC (minus end trap; Fig. 2, A4–A6 and A8; and see Fig. 8).

Accumulation of fluorescently labeled vesicles within the cut end of the axon

To examine the distribution kinetics of vesicles after axotomy in relation to the restructuring of MT cytoskeleton, we labeled the MTs by EB3-GFP and labeled membrane-bound organelles by the styryl dye RH237 (Grinvald et al., 1982; Sahly et al., 2006). The labeling procedure was performed as follows: mRNA encoding EB3-GFP was injected into neurons that were cultured

4–6 h earlier, and the neurons were immersed for 30 min in RH237. Initially, RH237 partitions into the plasma membrane (Malkinson and Spira, 2006; Sahly et al., 2006); thereafter, the dye is internalized by membrane retrieval and labels endocytotic vesicles. 12–24 h later, RH237 fluorescence is further distributed among membrane-bound organelles, as indicated by correlations between the fluorescence labeling and electron microscope observations (Sahly et al., 2006). Thus, using this protocol, RH237 indiscriminately labels lipid membranes of both anterogradely and retrogradely transported organelles.

As soon as MT polarity is reorganized after axotomy (Fig. 2, A1–A8), RH237 fluorescence begins to accumulate within the plus end trap and, to a lesser extent and more slowly, along the minus end trap (Fig. 2, B1–B8 and C1–C8; and Videos 2 and 3, available at http://www.jcb.org/cgi/content/full/jcb.200607098/DC1). To establish that the accumulated RH237 signal represents the accumulation of vesicles, we compared the distribution of RH237 fluorescence with the ultrastructural composition of the axon at various times after axotomy ($n > 10$) and confirmed that the RH237 fluorescence signal localizes at regions in which the vesicles and tubular structures concentrate (Sahly et al., 2006).

Sorting of anterogradely transported Golgi-derived vesicles from retrogradely transported pinocytotic vesicles

Labeling of subcellular organelles by RH237 revealed the presence of two distinct zones at which vesicles accumulate (the GCOC and the DZ). However, as RH237 labels lipids in general, it did not allow differentiation between anterogradely and retrogradely transported vesicles. Therefore, we specifically labeled anterogradely transported vesicles using intracellular injections of mRNA encoding superecliptic synaptopHluorin (Sankaranarayanan et al., 2000), enhanced YFP (EYFP)–SNAP-25 (25-kD synaptosome-associated protein; Oyler et al., 1989; Kimura et al., 2003), or cherry (Shaner et al., 2004) –SNAP-25 4–6 h before axotomy and imaging. Retrogradely transported pinocytotic vesicles were labeled by bath application of the fluid-phase pinocytotic maker sulforhodamine 101 (SR101; Teng et al., 1999). In a series of control experiments, we established that (1) the injection of mRNA encoding enhanced GFP, EYFP, or cherry leads to an evenly distributed fluorescent signal that does not concentrate in any of the traps after axonal transection. (2) Vesicles labeled by synaptopHluorins, EYFP–SNAP-25, or cherry–SNAP-25 4–6 h before axotomy are almost exclusively transported anterogradely (Videos 4 and 5, available at http://www.jcb.org/cgi/content/full/jcb.200607098/DC1), and vesicles labeled by SR101 are transported retrogradely (Video 6).

To illustrate the differential accumulation of anterogradely and retrogradely transported vesicles into the plus and minus end traps, we show simultaneous imaging of the anterogradely transported EYFP–SNAP-25 (Fig. 3 B), the retrogradely transported SR101 (Fig. 3 C), and the distribution of RH237 (Fig. 3 A). For the experiment ($n > 20$), we first labeled the entire population of vesicles by 30-min incubation of the neuron in RH237; 20 h

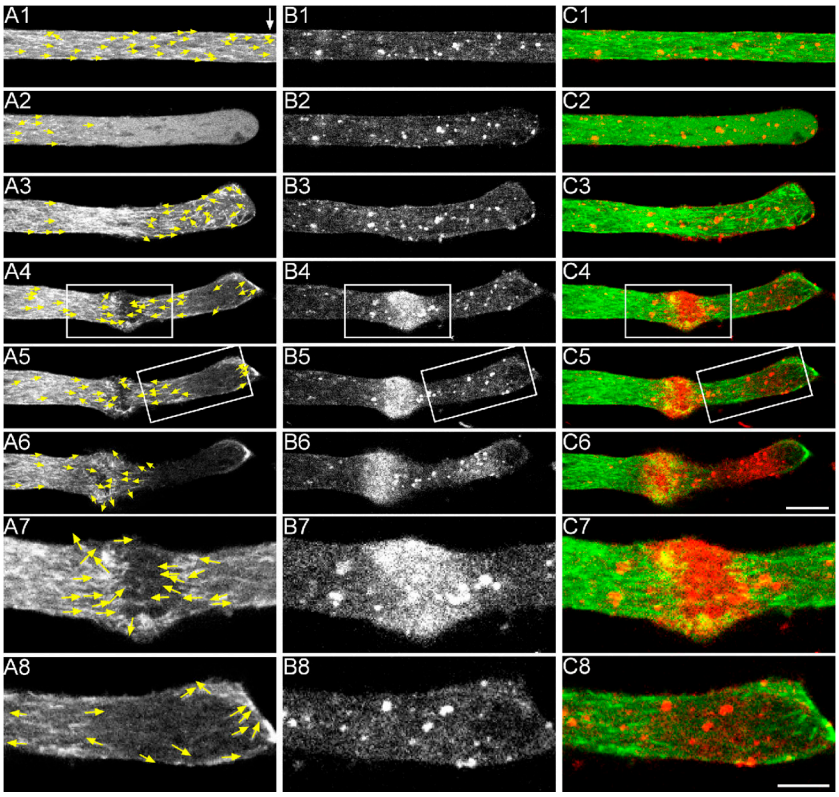

Figure 2. **Restructuring of MTs after axotomy.** (A–C) A B neuron was cultured for 4 h and microinjected with EB3-GFP mRNA. 1 h later, the neuron was bathed in RH237 for 30 min. The experiment began 16 h later by online imaging of the distribution of the EB3-GFP signal (A) and RH237-labeled vesicles (B) 3 μm above the substrate. Merged images of EB3-GFP (green) and RH237 (red) fluorescent signals are shown in C. Yellow arrows indicate the plus ends of the MTs as revealed by online imaging of the EB3-GFP signals. (A1) Before axonal transection (control; the site of axotomy is indicated by a white arrow), all of the MT plus ends point toward the tip of the axon. (B1) The RH237-labeled vesicles are distributed in the axoplasm. (C1) The merged image of A1 and B1. (A2) Axotomy leads within seconds to depolymerization of the MTs as indicated by dissipation of the EB3-GFP comet tail structures. (B2 and C2) Distribution of the RH237 fluorescence was unaltered. Within minutes of axotomy, the MTs repolymerize, and EB3-GFP reappears. However, in contrast to the control (A1), the plus ends of the MTs at the DZ point in various directions (arrows in A3). (B3) This is not associated with any noticeable change in the distribution of the RH237 signal. Within the next 10 min, the MTs reorient to form a plus end trap (boxed area in A4, which is enlarged in A7) and a minus end trap (boxed area in A5, which is enlarged in A8). The formation of the traps is associated with accumulation of the RH237 fluorescent signal mainly in the plus end trap (boxed area in B4, which is enlarged in B7) and, to a lesser extent, in the minus end trap (boxed area in B5, which is enlarged in B8). The corresponding merged images are shown in C4, C7, C5, and C8. The number of MTs that form the traps increases with time, as does the accumulation of RH237-labeled vesicles. Images were taken after axotomy as follows: A1–C1, control; A2–C2, 6 s; A3–C3, 1 min; A4–C4, 7 min; A5–C5, 9 min; A6–C6, 19 min. Bars (A1–C6), 10 μm; (A7–C8), 5 μm. Corresponds to Videos 1–3 (available at http://www.jcb.org/cgi/content/full/jcb.200607098/DC1).

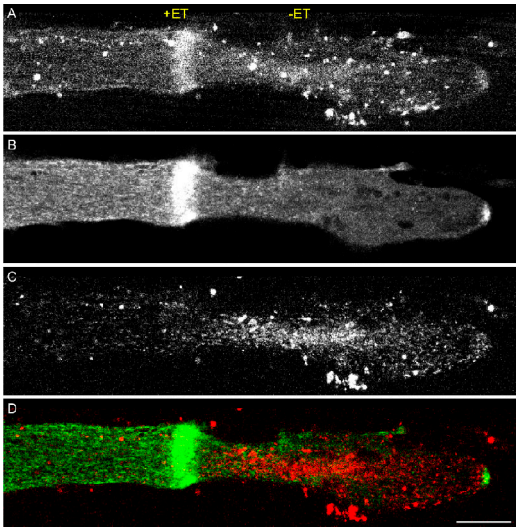

Figure 3. **Differential accumulation of anterogradely transported vesicles labeled by SNAP-25 and retrogradely transported vesicles labeled by the pinocytotic marker SR101.** A B neuron was cultured for 4 h. To label membrane-bound organelles, the neuron was bathed in RH237 for 30 min. 24 h later and 4 h before the axon was transected, EYFP–SNAP-25 mRNA was microinjected into the neuron. To label endocytotic vesicles, the neuron was incubated for 20 min in SR101. Images taken 20 min after axotomy are shown. (A) The spatial distribution of RH237-labeled vesicles corresponds to the plus (+ET) and minus end (−ET) vesicle traps. (B) Anterogradely transported EYFP–SNAP-25 fluorescence concentrates in the region of the plus end trap and at the very tip of the axon. (C) Vesicles labeled by SR101 are retained in the DZ. (D) The merged image of EYFP–SNAP-25 (green) and SR101 fluorescence (red) demonstrates their differential accumulation in the plus and minus end traps, respectively. Bar, 15 μm.

later, (i.e., 4 h before axotomy), the neuron was injected with mRNA encoding EYFP–SNAP-25. Subsequently, 2 h before transection, the neuron was exposed for 20 min to the pinocytotic marker SR101. After axotomy, under such conditions, anterogradely transported EYFP–SNAP-25–labeled vesicles specifically concentrate within the GCOC (Fig. 3 B), and the retrogradely transported pinocytotic vesicles labeled by SR101 were retained at the DZ (Fig. 3 C). The merged image of both labeling patterns closely matches that of the distribution of RH237 (Fig. 3, compare A with D). As a complementary approach, we also performed experiments in which we simultaneously imaged EB3-GFP and cherry–SNAP-25 or EB3-GFP and SR101. In these experiments, we also observed that anterogradely and retrogradely transported vesicles concentrate in the plus end trap (Fig. 4 B and Video 7, available at http://www.jcb.org/cgi/content/full/jcb.200607098/DC1) and minus end trap (Fig. 5 A and Video 9), respectively. Together, these observations demonstrate that the traps formed by MTs lead to the sorting and concentration of vesicles in accordance with their directional movement along MTs.

An understanding of the mechanisms that underlie the reversal of MT polarity and the formation of traps

We next began to explore the mechanisms that underlie formation of the plus and minus end vesicle traps. First, we examined whether molecular components associated with anterograde- or retrograde-transported vesicles generate the initial forces to reverse the polarity of the repolymerizing MTs. To that end, we reduced the supply of anterograde-transported vesicles and molecular constituents by removal of the cell body from the axon. It should be noted that isolated distal axonal segments of cultured *A. californica* neurons maintain their structure, fire action potentials, and even release neurotransmitters for several days (Benbassat and Spira, 1993; Benbassat and Spira, 1994; Martin et al., 1997; Oren et al., 1997; Schacher and Wu, 2002). The experiments described in the next paragraph (Figs. 4 and 5) were conducted 5 min–4.5 h after axonal isolation, which is well within a window of time in which many of the cellular functions of the isolated axon are operating quite normally.

For the experiments, the cell body together with a short axonal segment was mechanically removed, leaving a long, isolated axon in the culture (first axotomy; Fig. 4 A2). After various time intervals, which we believe allowed for depletion of the anterogradely transported components from the main axon, the isolated axon was transected again distally to the first transection (second axotomy; Fig. 4 A3). The restructuring of MTs and accumulation of anterogradely or retrogradely transported vesicles under these conditions were then imaged (Figs. 4 and 5, respectively).

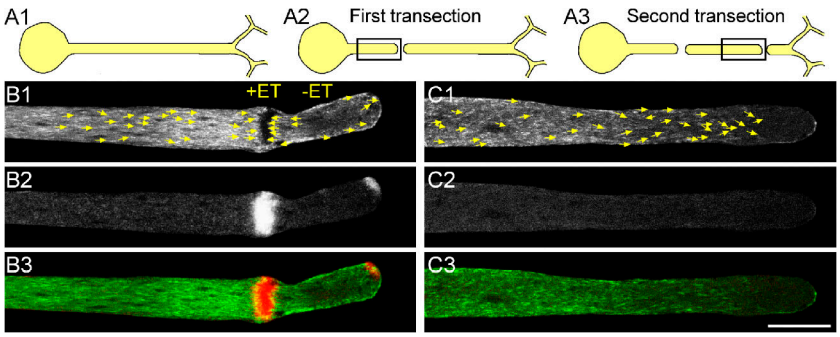

Figure 4. **Formation of the MT-based plus and minus end traps depends on the anterograde transport of component from the cell body to the axon.** A B neuron was cultured for 4 h and microinjected with EB3-GFP. Approximately 17 h later, the neuron was injected with cherry–SNAP-25 mRNAs. (A1 and A2) 5 h later, the axon was transected (first transection), and the distribution of EB3-GFP and cherry–SNAP-25 were imaged. (B1–B3) Images taken 5 min after axonal transection 3 μm above the substrate are shown, which corresponds to the boxed area in A2. Arrows in B1 indicate plus ends of the MTs as revealed by EB3-GFP imaging. Note the formation of the plus end (+ET) and minus end traps (−ET). (B2) The cherry–SNAP-25 fluorescent signal concentrated within the plus end trap and at the tip of the axon. (B3) A merged image of B1 (green) and B2 (red). (C1–C3) 3 h after the first transection, the isolated axon was transected again (A3; second transection). The images were taken 18 min after the transection from an area corresponding to the box in A3. Note that even 1 h after axotomy, the MT polarity was unchanged (arrows in C1 indicate the plus ends), and the cherry–SNAP-25 fluorescent signal did not accumulate (C2). (C3) a merged image of C1 (green) and C2 (red). Bar, 20 μm. Corresponds to Videos 7 and 8 (available at http://www.jcb.org/cgi/content/full/jcb.200607098/DC1).

MTs were imaged by EB3-GFP, and anterogradely transported vesicles were imaged by cherry–SNAP-25 or synaptopHluorins (Figs. 4 and 6 and Videos 7 and 8, available at http://www.jcb.org/cgi/content/full/jcb.200607098/DC1). Retrogradely transported vesicles were imaged by SR101 (Fig. 5 and Videos 9 and 10). In a series of 34 experiments in which we first imaged the formation of vesicle traps after axotomy of an intact neuron (first axotomy) and then imaged cytoskeleton reorganization after axotomy of the isolated axon (second axotomy) at different time intervals, we found that in 27/34 experiments, the cut end of the isolated axons (second axotomy) did not form the vesicles traps. However, as indicated by EB3 labeling, the MTs underwent a cycle of depolymerization and repolymerization in response to the second axotomy (Fig. 4 C1, Fig. 5 B1, and Videos 8 and 10). In these experiments, anterogradely transported vesicles did not accumulate (Fig. 4, C2 and C3; and Video 8). These results show that anterogradely transported molecular components, which are driven from the cell body to the axon, participate in the formation of traps.

An additional explanation to the aforementioned results could be that the accumulation of retrograde vesicles and associated proteins in the DZ participates in the formation of traps. According to this hypothesis, one could argue that the isolation of an axon from the cell body not only leads to the depletion of anterograde components but also retrograde components. To evaluate this hypothesis, intact neurons were bathed in SR101 solution for 20 min. 40–60 min after removal of the dye, the neuron was axotomyzed (first axotomy; $n = 7$; Fig. 5 A and Video 9). Within seconds of axotomy and in parallel to depolymerization of the MTs, retrograde transport of the SR101-labeled vesicles stops along the DZ (Fig. 5 A2 and Video 9). In contrast, the retrograde transport of vesicles within the PZ (in which the MTs maintain normal organization) continued, and, thus, within minutes of axotomy, almost all SR101-labeled vesicles cleared away from the PZ but were retained in the DZ (Fig. 5 A2). SR101-labeled vesicles transiently trapped within the forming plus end trap were driven out of the GCOC (Video 9). Using the same SR101 loading procedure, we found that axons that were isolated from their cell bodies for 5 min–4.5 h maintained retrograde transport of SR101-labeled vesicles. Second axotomy of such isolated axons leads to the immediate cessation of SR101 transport within the DZ as in the control experiments. Because the isolated axon is too short, we could not image the removal of the vesicles proximally from the PZ (Fig. 5 B and Video 10). The behavior of the retrogradely transported vesicles indicates that even 4.5 h after the first axotomy, retrogradely transporting motors are still present in the main axon. Collectively, the aforementioned results suggest that formation of the plus and minus end vesicle traps depends on the supply of anterogradely transported organelles or other molecular factors from the cell body to the cut axonal end.

To differentiate between the possibilities that Golgi-derived vesicles and tubules or anterogradely transported molecular motors and proteins underlie the trap formation, we disrupted the Golgi system by incubating the neurons for 12 h in 10 μg/ml brefeldin A (BFA; Chardin and McCormick, 1999). (It should be noted that in cultured *A. californica* neurons, 10 μg/ml BFA disrupts the Golgi apparatus within 30 min of application). Thereafter, neurons expressing EB3-GFP, EYFP–SNAP-25, or cherry–SNAP-25 were transected and imaged ($n = 17$). We found that both the plus and minus end traps are formed in the presence of BFA (Video 11, available at http://www.jcb.org/cgi/content/full/jcb.200607098/DC1), whereas SNAP-25–labeled anterogradely transported vesicles are not detected along the axon and do not accumulate in the traps (see Fig. 7 and Video 11). These observations suggest that formation of the traps does not require the arrival of Golgi-derived anterogradely transported vesicles but requires other anterogradely transported molecular signals.

We next attempted to examine whether retrogradely or anterogradely oriented molecular motors or cytoplasmic dynein and kinesin, respectively, generate the initial forces to form the vesicle traps. Unfortunately, most of our attempts to use pharmacological tools to inhibit the molecular motor proteins did not prove useful. For example, injection of cytoplasmic dynein inhibitor sodium ortovanadate (Gibbons et al., 1978) into the neurons led to drastic shortening of the EB3- GFP comet tails to a point that we could no longer follow the MT polarity. Bath application of 5 mM vanadate for 3 h or injection of antidynein antibodies (Santa Cruz Biotechnology, Inc.) did not inhibit retrograde transport. However, bath application of 2–3 mM dynein inhibitor erythro-9-(2-hydroxy-3-nonyl)adenine (EHNA; Bouchard et al., 1981; Goldberg, 1982; Ekstrom and Kanje, 1984) for 1–3 h inhibited the retrograde transport of SR101-labeled vesicles (Fig. S1, available at http://www.jcb.org/cgi/content/full/jcb.200607098/DC1)

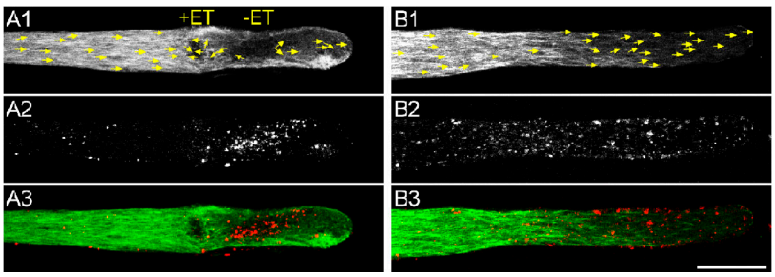

Figure 5. **Formation of the MT-based plus and minus end traps cannot be correlated with retrogradely transported retrieved membrane.** A B neuron was cultured for 4 h and microinjected with EB3-GFP mRNA. 18 h later, the neurons were incubated for 20 min in a solution containing the fluid-phase endocytotic marker SR101. The excess dye was washed away, and the axon was transected 1 h later, as shown in Fig. 4 (A1 and A2; first transection). (A) Imaging revealed that axotomy leads to formation of the plus and minus end traps (A1; +ET and –ET, respectively) and that SR101 concentrates in the minus end trap and is cleared away from the plus end trap and PZ by transport (A2). A3 is the merged image of A1 (green) and A2 (red). 3 h after the first transection, the isolated axon was exposed again to SR101 and transected (Fig. 4 A3; second transection). (B2) Note that the presence of vesicles that are carried retrogradely in the DZ is insufficient to induce the formation of the traps. The images in A were taken 10 min after the first transection, and those in B were taken 19 min after the second transection. Arrows in A1 and B1 indicate the plus ends of the MTs. Bar, 20 μm. Corresponds to Videos 9 and 10 (available at http://www.jcb.org/cgi/content/full/jcb.200607098/DC1).

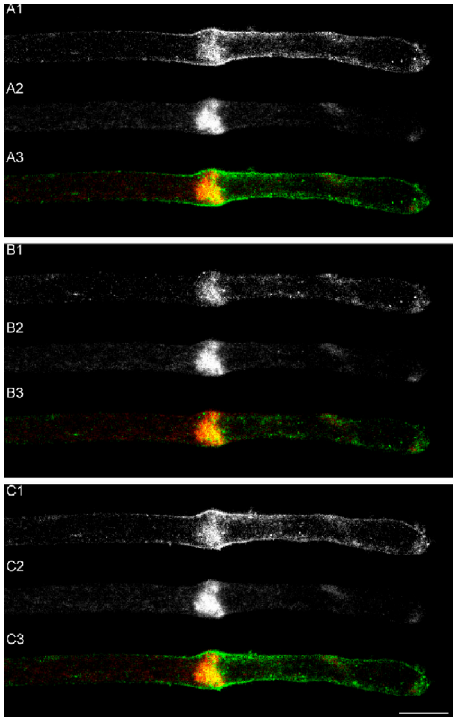

Figure 6. **Accumulation and fusion of Golgi-derived vesicles with the GCOC plasma membrane.** A buccal neuron was cultured for 12 h and microinjected with superecliptic synaptopHluorin mRNA. 4.5 h later, the axon was transected, and the synaptopHluorin signal was imaged using 405- (A2, B2, and C2) and 488-nm (A1, B1, and C1) excitation lasers. A3, B3, and C3 are the merge images of A1, B1, and C1 (green) and A2, B2, and C2 (red). (A1–A3) 10 min after axotomy, the 405-nm signal accumulates within the GCOC. The 488-nm signal is detected within the GCOC domain and on the plasma membrane surrounding it. (B1–B3) Pressure ejection of acidic solution (pH 5.4) on to the GCOC caused a sharp drop of the 488-nm signal located on the plasma membrane but not within the GCOC. The 405-nm signal was not influenced by this procedure. (C1–C3) Upon termination of the application, the 488-nm signal recovered. The images were taken 3 μm above the substrate level. Bar, 15 μm.

but did not inhibit formation of the vesicle traps. These observations suggest that retrogradely oriented molecular motors do not contribute to formation of the traps. We then examined the hypothesis that anterogradely transported kinesin motors contribute to the trap formation. To that end, we microinjected the nonhydrolyzable analogue of ATP (adenosine 5′-[β,γ-imido]triphosphate– AMP-PNP) as a kinesin inhibitor (Kapoor and Mitchison, 1999; Bananis et al., 2000) and found that in addition to blocking the axoplasmic transport and inhibition of vesicle trap formation after axotomy, it increased the free intracellular calcium levels (as imaged with fura-2) and subsequently led to axonal degeneration. Microinjection of antikinesin antibody (monoclonal mouse antibovine brain kinesin heavy chain; Chemicon) into the neurons did not inhibit anterograde transport and had no effect on formation of the traps.

GC extension after axotomy depends on the accumulation of Golgi-derived vesicles in the GCOC

Subdivision of the cut axonal end into a spatially and functionally distinct plus end trap, which concentrates Golgi-derived membrane resources from the PZ and DZ that continuously retrieve plasma membrane, may enable the extension of a GC lamellipodium on a background of dominating membrane retrieval (Ashery et al., 1996). To evaluate the validity of this hypothesis, we examined (1) whether the vesicles within the GCOC fuse with the plasma membrane and (2) whether the prevention of anterogradely transported vesicle accumulation at the GCOC is sufficient to prevent the extension of a GC's lamellipodium.

The fusion of vesicles that are anterogradely transported and accumulate in the GCOC with the plasma membrane to form the nascent GC was confirmed by injection of mRNA encoding superecliptic synaptopHluorin (Miesenbock et al., 1998) into the cell body 2–5 h before axotomy. The neuron was then axotomized and formed a GCOC. Imaging of synaptopHlourin-labeled vesicles by excitation wavelength of 405 nm revealed the accumulation of vesicles within the GCOC (Fig. 6, A2, B2, and C2). To examine whether these vesicles fuse with the plasma membrane, we imaged the synaptopHluorin-labeled structures by excitation wavelength of 488 nm. This excitation wavelength exclusively activates synaptopHluorins in neutral pH environments (i.e., facing the culture medium). These images revealed that most of the fluorescent signal is localized to the plasma membrane around the GCOC, and part of it is detected within the GCOC cytoplasm (Fig. 6, A1, B1, and C1). These signals are generated by vesicles that fused with the plasma membrane and face the neutral pH of the medium and organelle population with intermediate internal pHs. Confirmation of these conclusions is provided by the experiment in Fig. 6. After control imaging of the GCOC (Fig. 6 A), an acidic culturing solution (pH 5.4) was pressure ejected onto the GCOC. This resulted in an immediate and reversible disappearance of most fluorescent signals generated by excitation at 488 nm from the GCOC's plasma membrane (Fig. 6, compare the A1 control with B1 and note the recovery in C1). These observations clearly demonstrate that anterogradely transported vesicles that concentrate within the GCOC fuse with the surrounding plasma membrane.

To examine whether Golgi-derived vesicles rather than retrieved vesicles are necessary for the promotion of axotomy-induced growth, the supply of anterogradely transported Golgi-derived vesicles was interrupted by bath application of 10 μg/ml BFA. We established that in the presence of BFA, GCs continue to extend for several hours (for as long as vesicles that were processed before BFA application were available; unpublished data). Thus, BFA does not inhibit the fusion of vesicles with the GC plasma membrane in a direct manner ($n = 5$). We next examined whether the depletion of Golgi-derived vesicles is sufficient to prevent GC formation after axotomy by first incubating the neurons for 12–15 h in 10 μg/ml BFA. Next, EYFP–SNAP-25 mRNA was injected into the cell body, and, 4 h later, the axon was transected. As indicated by the presence of diffuse EYFP fluorescent signal in the axon, we conclude that the injected mRNA was translated (Fig. 7 B). Nevertheless, the fluorescent signal did not concentrate in the GCOC (Fig. 7 B), and a GC lamellipodium did not extend (Fig. 7 A). SR101 imaging revealed that membrane retrieval proceeds normally in the presence of BFA (unpublished data) and that retrogradely transported

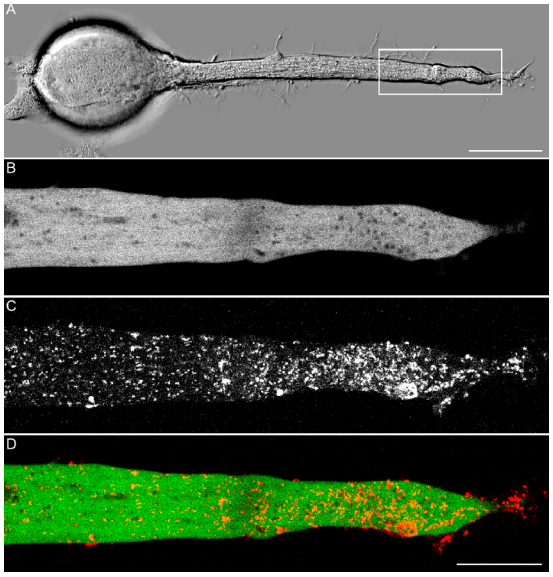

Figure 7. **Regeneration of the cut axonal end depends on the accumulation of Golgi-derived vesicles in the GCOC and not on retrieved retrogradely transported vesicles.** 10 μl/ml BFA was added to the bathing solution of a B neuron. 15 h later, the neuron was injected with EYFP–SNAP-25 mRNA. 1 h before axonal transection, the neuron was exposed for 20 min to SR101 and was transected. Images were taken 3 μm above the substrate level from the boxed area indicated in A. (A) Transmitted light micrograph taken 40 min after axotomy shows that the axon failed to regenerate a GC's lamellipodium. (B) As indicated by the fluorescent signal, the injected EYFP–SNAP-25 mRNA was translated in the presence of BFA. Nevertheless, the signal was distributed along the axon rather than accumulating within the GCOC, as in the control experiments. This result is consistent with the fact that the Golgi apparatus disintegrates in the presence of BFA. (C) The SR101 fluorescent signal was retained within the DZ as in the control experiments. (D) A merge image of B (green) and C (red). B–D were taken 28 min after axotomy. Bars (A), 100 μm; (B–D) 20 μm.

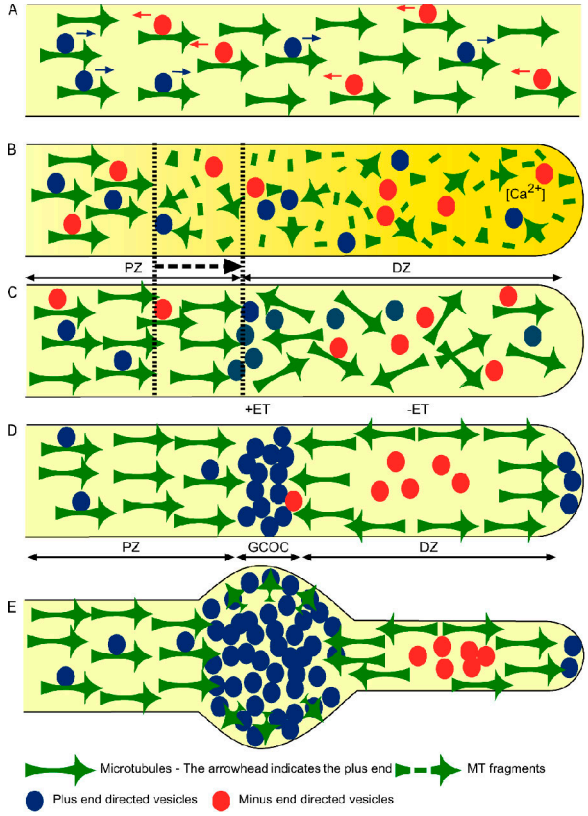

Figure 8. **Diagrammatic summary of the structural events leading to the formation of MT-based plus and minus end vesicle traps after axotomy.** (A) In intact neurons, the MTs orient their plus end distally (arrows) toward the tip of the axon. Anterograde (blue) and retrograde (red) vesicles are transported along the MTs. (B) Axotomy leads to a calcium-dependent retrograde wave of MT depolymerization along a neuronal segment of ~50–100 μm (yellow gradient). Concomitantly, the vectorial motion of transported vesicles along the distal segment stops. The MT depolymerization wave ends when the free intraaxonal calcium concentration recovers to its resting level. (C) This is followed within minutes of axotomy by repolymerization of the MTs in two forms: a directional anterograde wave of MT repolymerization from the PZ toward the DZ (dashed arrow) and repolymerization of MTs in all directions in the distal segment of the cut axon (DZ). (D) Within minutes, the polarity of the MTs is restructured: in the PZ, all MTs point their plus ends anterogradely. Retrogradely transported vesicles (red) continue their journey and, thus, are cleared away from this region. In contrast, the vectorial transport of plus end–driven vesicles continues, and the anterogradely driven vesicle concentration increases at this interface. (D and E) Distal to it and in relation to the local concentration of anterogradely transported vesicles, the orientation of the MTs reverses such that the plus ends point retrogradely. (D) This reversal of MT orientation creates the narrow GCOC, which is bordered both proximally and distally by the MT plus ends. Distal to the GCOC, the MT plus ends point toward the plasma membrane at the tip of the cut axon or are aligned in parallel and close to the plasma membrane. This MT orientation forms a second zone, which is bordered by the minus end of the MTs. This MT configuration traps in the center minus end–driven vesicles (red) and sends away toward the very tip of the axon vesicles that are driven by plus end–oriented motors (D, blue). (E) With time, the structure becomes more robust, and the subdivision to PZ, GCOC, and DZ becomes more visible.

vesicles are retained by the minus end trap (Fig. 7, C and D), but the formation of a GC's lamellipodium is inhibited. Because of this, we conclude that the accumulation of Golgi-derived vesicles within the plus end trap is essential for promoting the rapid regenerative pattern after axotomy.

Discussion

This study demonstrates that axotomy of cultured *A. californica* neurons leads to rapid reorganization of the MT skeleton at the tip of the transected axon to form two distinct vesicle traps (Fig. 8). These include a proximal trap (the plus end trap), which is located some 50–150 μm from the reformed axonal end, and a distal trap (the minus end trap), which is situated in between the proximal trap and the reformed end (Fig. 8). The plus end trap concentrates vesicles that are anterogradely transported along MT tracks by plus end–directed molecular motors and sends away cargo that is driven by minus end–directed motors. The minus end trap retains retrogradely transported vesicles and sends away cargo that is driven by plus end–directed motors. The efficient concentration of Golgi-derived vesicles that fuse with the plasma membrane enables the extension of a GC's lamellipodium from the GCOC. When the supply of Golgi-derived vesicles is interrupted, a GC lamellipodium is not formed (Fig. 7). The retention of retrogradely transported vesicles by the minus end trap at the DZ (Spira et al., 2003; Sahly et al., 2006) and the concentration of anterogradely transported vesicles by the plus end trap at the GCOC may serve to prevent mixing of freshly supplied vesicles and retrieved vesicles. Thus, formation of the traps enables the neuron to locally allocate

membrane resources for the effective extension of a GC lamellipodium after axotomy on a general background of a quantitatively dominating membrane retrieval regime (Ashery et al., 1996). In summary, the formation of MT-based vesicle traps optimizes growth processes by sorting and concentrating Golgi-derived membrane resources at a restricted site in the cut axon.

Proposed mechanism for trap formation

Based on our observations and supported by extensive studies of the mechanisms underlying the organization of polar MT arrays in mitosis, the transport of pigment granules in cytoplasmic fragments of melanophores, and cytoplasmic streaming (Cytrynbaum et al., 2004; Serbus et al., 2005), we propose the following model for the formation of MT-based traps (Fig. 8). Axotomy is followed by Ca^{2+} influx into the axoplasm through the cut axonal end (Ziv and Spira, 1995, 1997; Spira et al., 2003). As indicated by time-lapse confocal imaging of tetramethyl-rhodamine tubulin–labeled MTs and electron microscopy, the $[Ca^{2+}]_i$ wave induces disassembly of the MTs (Spira et al., 2003; Sahly et al., 2006). Initially after axotomy, two distinct zones of MTs are formed by the retrograde Ca^{2+} wave: the DZ, in which the MTs are depolymerized or fragmented, and a PZ, in which the MTs are not affected (Fig. 8 B; Spira et al., 2003; Sahly et al., 2006). Within minutes of $[Ca^{2+}]_i$ recovery, the MTs of the PZ repolymerize in a proximo-distal direction (Sahly et al., 2006), and the dissociated MTs within the DZ repolymerize (Fig. 8 C and Video 1). At first, the repolarized MTs point their plus ends in various directions within the axoplasm of the DZ (Fig. 8 C), the orientations of the MTs change, and distinct plus and minus end traps are formed (Fig. 8, D and E).

Our results support the hypothesis that reorientation of MT polarity to form the vesicle traps depends on the supply of anterogradely transported molecular components from the cell body to the site of injury. Thus, when an axon is isolated for $>$.5 h from the cell body, axotomy is not followed by formation of the plus and minus end traps. Rather, the MTs repolymerize with their plus ends pointing toward the tip of the cut axon (Figs. 4 C and 5 B and Videos 8 and 10). Because it is well established that isolated *A. californica* axons in culture maintain their normal morphology, generate action potentials, and even release neurotransmitters for $>$24 h (Benbassat and Spira, 1993, 1994; Martin et al., 1997; Oren et al., 1997; Schacher and Wu, 2002), it is reasonable to assume that the aforementioned observations, which were conducted within minutes to 4.5 h after axotomy, are not affected by a general rundown of the axon. We suggest that isolation of the axon from the cell body leads to the depletion of anterogradely transported molecular components that take part in formation of the vesicle traps.

Motor proteins as candidates for vesicle trap formation and maintenance

Previous studies suggested that the formation of polarized MT assemblies can be induced by a variety of cellular structures and molecules, such as membrane compartments, vesicles, cortical and cytoskeletal elements, Rho GTPases, receptors, and molecular motors (Gundersen et al., 2004; Akhmanova and Hoogenraad, 2005; Wu et al., 2006). Radial MT arrays are generally formed by the centrosome, which can induce the outgrowth of MTs with their plus ends directed outwards (Akhmanova and Hoogenraad, 2005). However, much evidence suggests that the centrosome-independent mechanism of MT organization is driven by molecular motors that can substitute for it (Malikov et al., 2005). In fish melanophores, the MT self-organization depends on the minus end–directed motor dynein and occurs through a combination of MT-based granule transport and MT nucleation on the pigment granules (Vorobjev et al., 2001). It was suggested that the dynein molecular complexes interact with more than one MT, and, while propagating toward the minus ends along two MTs, the dynein complex forces the MT plus ends to orient away from the motor (Vorobjev et al., 2001; Cytrynbaum et al., 2004; Malikov et al., 2005). Assuming that dynein remains attached to the MT when it reaches the minus end, the final orientations of the MTs are stabilized such that all minus ends are attached to the dynein complex and all plus ends point away from it. Similar arguments were considered regarding kinesin motors (Serbus et al., 2005).

We found that the inhibition of retrogradely transported SR101-labeled vesicles by EHNA does not interfere with trap formation (Fig. S1). Although this observation cannot rule out with certainty that dyneins are involved in trap generation, the results indicate that formation of the plus and minus end vesicle traps depends on the supply of anterogradely transported molecules from the cell body to the cut axonal end. Because BFA treatment, which disrupts the Golgi apparatus and thus blocks the supply of Golgi-derived vesicles, did not block MT trap formation, we concluded that the restructuring of MT polarity at the cut axonal end is generated by anterogradely transported signals such as the molecular motors themselves or other protein signals (Vorobjev et al., 2001; Cytrynbaum et al., 2004; Serbus et al., 2005).

The results presented in this study suggest but do not prove that plus end–directed molecular motors serve to power the formation of the plus end trap by their accumulation at the severed tips of MTs (Fig. 8, C–E). This process may also contribute indirectly to formation of the minus end trap. This trap is bordered on one side by the minus ends of the MTs that point their plus ends toward the center of the plus end trap (Fig. 8). On the other side of the minus end trap, the MTs point their plus ends toward the plasma membrane. Similar reactions have been demonstrated in both yeast and mammalian cells in which MT stabilization is caused by the interaction of a MT's plus end and proteins localized at the plasma membrane (Allan and Nathke, 2001; Akhmanova and Hoogenraad, 2005). We hypothesize that with time, the trap structures become more robust as the polarity of the MTs direct more proteins and vesicles into the trap, and, as a consequence, more MTs assemble to fit the pattern. Thus, the self-assembled trap structure is reinforced, and the structural and functional subdivision of the cut end into the plus and minus end traps becomes more robust.

The functional role of the vesicle traps and its general implications

An earlier study from our laboratory revealed that the axotomy of cultured *A. californica* neurons activates membrane retrieval

and exocytosis in parallel. Membrane capacitance measurements revealed that the processes of membrane internalization quantitatively dominate exocytosis. Nevertheless, the neuron vigorously extends a GC's lamellipodium (Ashery et al., 1996). This apparent discrepancy is reconciled by assuming spatial dissociation between the site at which Golgi-derived vesicles accumulate and are being inserted into the plasma membrane and the sites from which the membrane is retrieved. It appears that formation of the two vesicle traps isolates the site of growth (GCOC) from the distal compartment that was exposed to very high calcium levels and initially undergoes massive membrane retrieval (Ashery et al., 1996; Fishman and Bittner, 2003). It also provides an efficient cellular mechanism to optimize the accumulation of growth-supporting vesicles and, thereby, facilitates localized growth processes.

It should be noted that earlier studies demonstrated that local disruption of MTs at the middle of an axonal segment either by nocodazole application (Zakharenko and Popov, 1998) or trypsin microinjection (Ziv and Spira, 1998) results in the insertion of transported membranes into the axonal membrane and the initiation of local growth. These observations could be interpreted to support the assumption that vesicles accumulate at the tips of disrupted MTs simply because they cannot move efficiently past that point. However, it is interesting to note that in a series of preliminary experiments (unpublished data), we found (using EB3-GFP) that trypsin microinjection, which leads to the generation of nascent GC extension, is preceded by the formation of a plus end vesicle trap within the middle of the axon. In light of the present findings, it would be interesting to examine with the right molecular tools whether the formation of MT-based vesicle traps serves similar functions in other neurons. It should be noted that the basic phenomenon and mechanisms that operate in generating vesicle traps in transected *A. californica* neurons have been previously described to serve a variety of functions in other cells (for review see Cytrynbaum et al., 2004).

Materials and methods

Solutions

Leibovitz's L-15 medium (Invitrogen) was supplemented for marine species (ms L-15) according to Schacher and Proshansky (1983) by the addition of 12.5 g/L NaCl, 6.24 g/L D(+) dextrose, 3.15 g/L anhydrous $MgSO_4$, 344 mg/L KCl, 192 mg/L $NaHCO_3$, 5.7 g/L $MgCl_2$-$6H_2O$, and 1.49 g/L $CaCl_2$-$2H_2O$. Penicillin, streptomycin, and amphotericin B (Biological Industries) were added to make final concentrations of 100 U/ml, 0.1 mg/ml, and 0.25 μg/ml, respectively. Culture medium consisted of 10% filtered hemolymph obtained from *Aplysia fasciata* (the specimens were collected along the Mediterranean coast) diluted in ms L-15. Artificial sea water consisted of 460 mM NaCl, 11 mM KCl, 10 mM $CaCl_2$, 55 mM $MgCl_2$, and 10 mM Hepes adjusted to pH 7.6.

Pharmacological reagents

RH237 (*N*-(4-sulfutyl)-4-(6-(p-dibutylamynophenyl) hexatrenyl)) pyridinum and inner salt (a gift from R. Hildeshiem, Weizmann Institute of Science, Rehovot, Israel; Grinvald et al., 1982) was diluted in ethanol to a concentration of 10 mM and further diluted before use in artificial sea water to a concentration of 10 μM. SR101 (Kodak) was prepared as a stock solution of 10 mM in double-distilled water and further diluted before use in artificial sea water to a final concentration of 40 μM. BFA (Sigma-Aldrich; Chardin and McCormick, 1999) was prepared as a stock solution of 5 mg/ml in methanol and was further diluted to a final concentration of 10 μg/ml in the experimental bathing solution. Retrograde transport of SR101-labeled vesicles was inhibited by bath application of EHNA and HCl (Calbiochem). For the experiments, EHNA was diluted in DMSO to a 1-M stock solution and was further diluted before use to final concentration of 2–3 mM in artificial sea water.

Cell culture

Neurons B1 and B2 from buccal ganglia of *A. californica* were isolated and maintained in culture as previously described (Schacher and Proshansky, 1983; Spira et al., 1993, 1996). In this study, we refer to these neurons collectively as B neurons. In brief, 1–10 g of juvenile *A. californica* supplied from the University of Miami's National Resource for *A. californica* was anesthetized by injecting 380 mM of isotonic $MgCl_2$ solution into the animal's body cavity. Buccal ganglia were dissected and incubated in ms L-15 containing 1% protease (type IX; Sigma-Aldrich) at 34°C for 1.5–2.5 h. After the protease treatment, the ganglia were pinned and desheathed. The neurons were manually pulled out along with their original axon with the aid of a sharp glass microelectrode. The neurons were immediately plated in glass-bottom dishes coated with poly-L-lysine (Sigma-Aldrich) containing culture medium. All experiments were performed 24–48 h after plating at room temperature (21–25°C) after replacing the culture medium with artificial sea water.

Axotomy

Axonal transection was performed by applying pressure on the axon with the thin shaft of a micropipette under visual control as previously described (Spira et al., 1993, 1996, 2003; Ziv and Spira, 1993).

mRNA preparation and injection

mRNAs were in vitro transcribed using the recombinant transcription system as described previously (Sahly et al., 2003). In brief, human protein plus EB3 was prepared as EB3-GFP (Stepanova et al., 2003), and *A. californica* SNAP-25 (provided by W.S. Sossin, Montreal University, Montreal, Canada) was prepared as EYFP–SNAP-25 or cherry–SNAP-25 (cherry was provided by R.Y. Tsien, University of California, San Diego, La Jolla, CA). These and superecliptic synaptopHluorin (provided by J.E. Rothman, Memorial Sloan-Kettering Cancer Center, New York, NY) were cloned in pCS2+ expression vector. 10 μg of those plasmids were linearized with NotI and purified using a DNA cleanup system (Promega). 1–3 μg of linearized DNA was transcribed using a RiboMax-sp6 kit (Promega). A typical reaction contains 8 μl of transcription buffer, 8 μl rNTP mix containing 25 mM CTP, ATP, UTP, and 12 mM GTP, 4 μl of 15 mM Cap analogue (Roche), 1 μl rRnasin (Promega), and 4 μl of enzyme mix. A final volume of 40 μl was incubated for 2–4 h at 37°C. RNA was purified by using an RNeasy Mini Kit (QIAGEN), and the clean RNA was eluted to a final volume of 25–40 μl and kept at –80°C until use.

The transcribed mRNAs were pressure injected into the cytoplasm of the cultured neurons 4–24 h after plating. In preparing the injections, 3 μl mRNA solution (0.5–5 μg/μl) was diluted in 0.5 μl KCl (0.5 M). We estimated the injected volume to be ~10% of the cell's body volume. Throughout the injection, the input resistance and transmembrane potential of the neuron were recorded by the injection micropipette. At the end of the injection, the micropipette was removed from the cell.

Microscope imaging

Two confocal imaging systems were used: the Radiance 2000/AGR-3 imaging system (Bio-Rad Laboratories) was mounted on an IX70 microscope (Olympus) with a plan-Apo 60X 1.4 NA oil objective (Olympus), and the D-Eclipse C1 imaging system (Nikon) was mounted on an Eclipse TE-2000 microscope (Nikon) with a plan-Apo 60X 1.4 NA oil objective (Nikon). SynaptopHluorin imaging was performed on the Nikon set. The protein was excited at 405 (blue diode laser) and 488 nm (argon laser). The emitted light was collected at 500–530 nm. Images were collected and processed using EZ-C1 software (Nikon). All other imaging was performed using the Bio-Rad Laboratories system. The images were collected and processed using LaserSharp and LaserPix software (Bio-Rad Laboratories), respectively. For simultaneous imaging of GFP fusion proteins and RH237, both chromophores were excited by 488 nm, and the emitted lights were collected at 500–530 nm for GFP and above 660 nm for RH237. For simultaneous imaging of GFP or EYFP fusion proteins and SR101 or cherry fusion proteins, the excitation wavelengths were 488 and 543 nm (green HeNe laser). The emission filter for GFP and EYFP was HQ 500–530 nm, and for SR101 and cherry, the filter was HQ 555–625 nm. Triple imaging of GFP- or EYFP-labeled proteins, SR101, and RH237 was collected by excitation wavelengths of 488 and 543 nm, and the emissions filters were HQ 500–530 nm for GFP or EYFP, HQ 560–580 nm for SR101, and HQ

660LP for RH237. The argon laser excitation intensity was usually lowered to 5–10%. The pinhole was set to 1.6–2.5 mm. Figures were prepared using Photoshop and FreeHand software (both from Adobe).

Online supplemental material

Fig. S1 shows that the effective inhibition of SR101-labeled vesicle retrograde transport by EHNA does not inhibit formation of the plus end trap. Videos 1–3 show the formation of MT-based vesicle traps after axotomy. Videos 4 and 5 show the anterograde transport of EYFP–SNAP-25–labeled vesicles and their accumulation after axotomy. Video 6 shows the retrograde transport of SR101-labeled vesicles. Videos 7 and 8 show that the formation of a plus end trap depends on the anterograde transport of components from the cell body to the axon. Videos 9 and 10 show that the formation of MT-based plus and minus end traps cannot be correlated with retrogradely transported retrieved membrane. Video 11 shows that the formation of MT-based plus and minus end traps does not depend on the supply of Golgi-derived anterogradely transported vesicles. Online supplemental material is available at http://www.jcb.org/cgi/content/full/jcb.200607098/DC1.

We thank Dr. E. Shapira and A. Dormann for technical help in preparing mRNAs and complementary electron microscope studies.

This study was supported by grants from the USA-Israeli Binational Science Research Foundation (grants 2000354 and 2003152). Parts of the work were performed at the Charles E. Smith Family and Prof. Elkes Laboratory for Collaborative Research in Psychobiology. M.E. Spira is the Levi DeViali Professor in Neurobiology.

Submitted: 19 July 2006
Accepted: 6 January 2007

References

Ahmad, F.J., Y. He, K.A. Myers, T.P. Hasaka, F. Francis, M.M. Black, and P.W. Baas. 2006. Effects of dynactin disruption and dynein depletion on axonal microtubules. *Traffic*. 7:524–537.

Akhmanova, A., and C.C. Hoogenraad. 2005. Microtubule plus-end-tracking proteins: mechanisms and functions. *Curr. Opin. Cell Biol.* 17:47–54.

Allan, V., and I.S. Nathke. 2001. Catch and pull a microtubule: getting a grasp on the cortex. *Nat. Cell Biol.* 3:E226–E228.

Ashery, U., R. Penner, and M.E. Spira. 1996. Acceleration of membrane recycling by axotomy of cultured *Aplysia* neurons. *Neuron*. 16:641–651.

Bananis, E., J.W. Murray, R.J. Stockert, P. Satir, and A.W. Wolkoff. 2000. Microtubule and motor-dependent endocytic vesicle sorting in vitro. *J. Cell Biol.* 151:179–186.

Benbassat, D., and M.E. Spira. 1993. Survival of isolated axonal segments in culture: morphological, ultrastructural, and physiological analysis. *Exp. Neurol.* 122:295–310.

Benbassat, D., and M.E. Spira. 1994. The survival of transected axonal segments of cultured *Aplysia* neurons is prolonged by contact with intact nerve cells. *Eur. J. Neurosci.* 6:1605–1614.

Bouchard, P., S.M. Penningroth, A. Cheung, C. Gagnon, and C.W. Bardin. 1981. erythro-9-[3-(2-Hydroxynonyl)]adenine is an inhibitor of sperm motility that blocks dynein ATPase and protein carboxylmethylase activities. *Proc. Natl. Acad. Sci. USA*. 78:1033–1036.

Chardin, P., and F. McCormick. 1999. Brefeldin A: the advantage of being uncompetitive. *Cell*. 97:153–155.

Cytrynbaum, E.N., V. Rodionov, and A. Mogilner. 2004. Computational model of dynein-dependent self-organization of microtubule asters. *J. Cell Sci*. 117:1381–1397.

Dai, J., and M.P. Sheetz. 1995. Axon membrane flows from the growth cone to the cell body. *Cell*. 83:693–701.

Ekstrom, P., and M. Kanje. 1984. Inhibition of fast axonal transport by erythro-9-[3-(2-hydroxynonyl)]adenine. *J. Neurochem.* 43:1342–1345.

Fishman, H.M., and G.D. Bittner. 2003. Vesicle-mediated restoration of a plasmalemmal barrier in severed axons. *News Physiol. Sci.* 18:115–118.

Gibbons, I.R., M.P. Cosson, J.A. Evans, B.H. Gibbons, B. Houck, K.H. Martinson, W.S. Sale, and W.J. Tang. 1978. Potent inhibition of dynein adenosinetriphosphatase and of the motility of cilia and sperm flagella by vanadate. *Proc. Natl. Acad. Sci. USA*. 75:2220–2224.

Goldberg, D.J. 1982. Microinjection into an identified axon to study the mechanism of fast axonal transport. *Proc. Natl. Acad. Sci. USA*. 79:4818–4822.

Grinvald, A., R. Hildesheim, I.C. Farber, and L. Anglister. 1982. Improved fluorescent probes for the measurement of rapid changes in membrane potential. *Biophys. J.* 39:301–308.

Gundersen, G.G., E.R. Gomes, and Y. Wen. 2004. Cortical control of microtubule stability and polarization. *Curr. Opin. Cell Biol.* 16:106–112.

Kapoor, T.M., and T.J. Mitchison. 1999. Allele-specific activators and inhibitors for kinesin. *Proc. Natl. Acad. Sci. USA*. 96:9106–9111.

Kim, T., and S. Chang. 2006. Quantitative evaluation of the mode of microtubule transport in *Xenopus* neurons. *Mol. Cells*. 21:76–81.

Kimura, K., A. Mizoguchi, and C. Ide. 2003. Regulation of growth cone extension by SNARE proteins. *J. Histochem. Cytochem.* 51:429–433.

Malikov, V., E.N. Cytrynbaum, A. Kashina, A. Mogilner, and V. Rodionov. 2005. Centering of a radial microtubule array by translocation along microtubules spontaneously nucleated in the cytoplasm. *Nat. Cell Biol.* 7:1213–1218.

Malkinson, G., and M.E. Spira. 2006. Calcium concentration threshold and translocation kinetics of EGFP-DOC2B expressed in cultured *Aplysia* neurons. *Cell Calcium*. 39:85–93.

Martin, K.C., A. Casadio, H. Zhu, E. Yaping, J.C. Rose, M. Chen, C.H. Bailey, and E.R. Kandel. 1997. Synapse-specific, long-term facilitation of aplysia sensory to motor synapses: a function for local protein synthesis in memory storage. *Cell*. 91:927–938.

Miesenbock, G., D.A. De Angelis, and J.E. Rothman. 1998. Visualizing secretion and synaptic transmission with pH-sensitive green fluorescent proteins. *Nature*. 394:192–195.

Nakagawa, H., K. Koyama, Y. Murata, M. Morito, T. Akiyama, and Y. Nakamura. 2000. EB3, a novel member of the EB1 family preferentially expressed in the central nervous system, binds to a CNS-specific APC homologue. *Oncogene*. 19:210–216.

Nguyen, M.P., G.D. Bittner, and H.M. Fishman. 2005. Critical interval of somal calcium transient after neurite transection determines B 104 cell survival. *J. Neurosci. Res.* 81:805–816.

Oren, R., A. Dormann, D. Benbassat, and M.E.D. Spira. 1997. Long term survival of isolated axonal segments as revealed by in vitro studies. *In* Neurochemistry: Cellular, Molecular, and Clinical Aspects. A. Teelken and J. Korf, editors. Plenum Press, New York. 647–653.

Oyler, G.A., G.A. Higgins, R.A. Hart, E. Battenberg, M. Billingsley, F.E. Bloom, and M.C. Wilson. 1989. The identification of a novel synaptosomal-associated protein, SNAP-25, differentially expressed by neuronal subpopulations. *J. Cell Biol.* 109:3039–3052.

Popov, S., A. Brown, and M.M. Poo. 1993. Forward plasma membrane flow in growing nerve processes. *Science*. 259:244–246.

Sahly, I., H. Erez, A. Khoutorsky, E. Shapira, and M.E. Spira. 2003. Effective expression of the green fluorescent fusion proteins in cultured *Aplysia* neurons. *J. Neurosci. Methods*. 126:111–117.

Sahly, I., A. Khoutorsky, H. Erez, M. Prager-Khoutorsky, and M.E. Spira. 2006. On-line confocal imaging of the events leading to structural dedifferentiation of an axonal segment into a growth cone after axotomy. *J. Comp. Neurol.* 494:705–720.

Sankaranarayanan, S., D. De Angelis, J.E. Rothman, and T.A. Ryan. 2000. The use of pHluorins for optical measurements of presynaptic activity. *Biophys. J.* 79:2199–2208.

Schacher, S., and E. Proshansky. 1983. Neurite regeneration by *Aplysia* neurons in dissociated cell culture: modulation by *Aplysia* hemolymph and the presence of the initial axonal segment. *J. Neurosci.* 3:2403–2413.

Schacher, S., and F. Wu. 2002. Synapse formation in the absence of cell bodies requires protein synthesis. *J. Neurosci.* 22:1831–1839.

Serbus, L.R., B.J. Cha, W.E. Theurkauf, and W.M. Saxton. 2005. Dynein and the actin cytoskeleton control kinesin-driven cytoplasmic streaming in *Drosophila* oocytes. *Development*. 132:3743–3752.

Shaner, N.C., R.E. Campbell, P.A. Steinbach, B.N. Giepmans, A.E. Palmer, and R.Y. Tsien. 2004. Improved monomeric red, orange and yellow fluorescent proteins derived from *Discosoma* sp. red fluorescent protein. *Nat. Biotechnol.* 22:1567–1572.

Spira, M.E., D. Benbassat, and A. Dormann. 1993. Resealing of the proximal and distal cut ends of transected axons: electrophysiological and ultrastructural analysis. *J. Neurobiol.* 24:300–316.

Spira, M.E., A. Dormann, U. Ashery, M. Gabso, D. Gitler, D. Benbassat, R. Oren, and N.E. Ziv. 1996. Use of *Aplysia* neurons for the study of cellular alterations and the resealing of transected axons in vitro. *J. Neurosci. Methods*. 69:91–102.

Spira, M.E., R. Oren, A. Dormann, and D. Gitler. 2003. Critical calpain-dependent ultrastructural alterations underlie the transformation of an axonal segment into a growth cone after axotomy of cultured *Aplysia* neurons. *J. Comp. Neurol.* 457:293–312.

Stepanova, T., J. Slemmer, C.C. Hoogenraad, G. Lansbergen, B. Dortland, C.I. De Zeeuw, F. Grosveld, G. van Cappellen, A. Akhmanova, and N. Galjart. 2003. Visualization of microtubule growth in cultured neurons via the use of EB3-GFP (end-binding protein 3-green fluorescent protein). *J. Neurosci.* 23:2655–2664.

Teng, H., J.C. Cole, R.L. Roberts, and R.S. Wilkinson. 1999. Endocytic active zones: hot spots for endocytosis in vertebrate neuromuscular terminals. *J. Neurosci.* 19:4855–4866.

Vorobjev, I., V. Malikov, and V. Rodionov. 2001. Self-organization of a radial microtubule array by dynein-dependent nucleation of microtubules. *Proc. Natl. Acad. Sci. USA*. 98:10160–10165.

Wu, X., X. Xiang, and J.A. Hammer III. 2006. Motor proteins at the microtubule plus-end. *Trends Cell Biol.* 16:135–143.

Yoo, S., J.E. Bottenstein, G.D. Bittner, and H.M. Fishman. 2004. Survival of mammalian B104 cells following neurite transection at different locations depends on somal Ca^{2+} concentration. *J. Neurobiol.* 60:137–153.

Zakharenko, S., and S. Popov. 1998. Dynamics of axonal microtubules regulate the topology of new membrane insertion into the growing neurites. *J. Cell Biol.* 143:1077–1086.

Ziv, N.E., and M.E. Spira. 1993. Spatiotemporal distribution of Ca2+ following axotomy and throughout the recovery process of cultured *Aplysia* neurons. *Eur. J. Neurosci.* 5:657–668.

Ziv, N.E., and M.E. Spira. 1995. Axotomy induces a transient and localized elevation of the free intracellular calcium concentration to the millimolar range. *J. Neurophysiol.* 74:2625–2637.

Ziv, N.E., and M.E. Spira. 1997. Localized and transient elevations of intracellular Ca^{2+} induce the dedifferentiation of axonal segments into growth cones. *J. Neurosci.* 17:3568–3579.

Ziv, N.E., and M.E. Spira. 1998. Induction of growth cone formation by transient and localized increases of intracellular proteolytic activity. *J. Cell Biol.* 140:223–232.